Experimental and Numerical Investigation of the Performance of Automotive Adhesively Bonded Crash Box Beams Under Transverse Loading

J. Bidadi[1], H. Hampaiyan Miandowab[1], H. Saeidi Googarchin[1*]

[1]Automotive Fluid and Structures Analysis Research laboratory, School of Automotive Engineering, Iran University of Science and Technology (IUST), Tehran, Iran

ARTICLE INFO	ABSTRACT
	The aim of the study was to examine the deformation modes and also degradation of an adhesively bonded rectangular cross section beam used in the automotive body structure. The study included: (1) performing new experimental investigations on the three-point bend behavior of a rectangular cross section beam made by adhesive bonding method. (2) developing a finite element (FE) model to predict the mechanical load displacement behavior and also the degradation modes (i.e. delamination between the adhesive layer and beam wall). The agreement between experimental and FE results demonstrates that the investigated structural element's numerical model was created utilizing accurate assumptions. Finally, the effects of beam wall thickness and overlap length have been investigated in a parametric study using the validated FE model. It was shown that increasing the beam wall thickness resulted in delamination between the adhesive layer and beam wall.

1. Introduction

Various joining methods can be utilized to assemble the automotive structural elements, including the mechanical joining techniques (such as fastening, welding, riveting, clinching, etc.), adhesive bonding, and also the hybrid joining processes that combine different types of mechanical and adhesive joints Simultaneously. The use of adhesives in the construction of automotive body structural elements has increased in recent years due to the many capabilities of the adhesive bonding method, such as reducing stress concentration by uniform stress distribution in the lap area and the capability of assembling dissimilar materials. The effectiveness of adhesive joints depends on several factors, including the geometry and material of the connecting elements (adherend) which include the shape and dimensions of the lap areas, the surface preparation method, and also the thickness of the adhesive layer and adherend materials. The majority of research papers only report on various experiments and modeling on simple adhesive joints, such as single-lap or double-lap joints [1-7]. However, in real structures, we typically encounter more cases, such as complex three-dimensional shapes of adherends, including thin-walled structures. Typical examples of these structures are thin-walled beams, columns, and profiles made of one or more thin-walled sheets joined together along an overlap length. Therefore, the effectiveness of the adhesive bonding method in these cases should be investigated as well. In recent years, the aerospace, marine, and automotive industries have paid close attention to the use of adhesive bonding methods for the construction of three-dimensional thin-walled beams with circular, rectangular, square, polygonal, C-shaped, I-shaped sections.

*Corresponding Author
Email Address: hsaeidi@iust.ac.ir
http://doi.org/10.22068/ase.2023.637

Experimental and Numerical Investigation of the Performance of Automotive Adhesively Bonded Crash Box Beams Under Transverse Loading

One of the most important issues in the assessment of three-dimensional adhesively bonded structures is the separation modeling of the connection or adhesive bonded area and its experimental verification. For instance, Sadowski et al. [8] conducted an experimental study of the effect of in-plane bending loads on mechanical behavior and bonding layer separation of an adhesively bonded beam with a hat-shaped cross-section used in the aerospace structures. To simulate the separation of adhesive bond area at the joint, they used a damage-based cohesive zone modeling (CZM) technique in the framework of the fracture mechanics approach [9]. Belingardi et al. [10] investigated the bending behavior of a composite/metal hybrid structure with a hat-shaped cross-section, as well as the effects of composite and metal location on top and bottom surface of beam on stiffness and energy absorption. Shin et al. [11] analysis the damage behavior of an aluminum/CFRP hybrid beam under three point bending by numerical and experimental methods. Delamination and debonding were modeled by a cohesive zone model (CZM) defined by the traction-separation law and an energy-based damage evolution scheme. Also, the employed fracture characteristics of the adhesive layer were measured experimentally by fracture mechanics concepts. In this paper, the applicability of the adhesive bonding method for the construction of rectangular-section automotive bumper beams under transverse quasi-static loads will be investigated using experimental and numerical methods. In the experimental scheme, the rectangular-section adhesively bonded beam is constructed through two steps: 1) plastic forming of the primary steel plate into two U-shape plates, 2) bonding the U-shape plates with a thin layer of adhesive. Subsequently, the fabricated beam is loaded under three-point bend quasi-static condition until a certain value of vertical cross-head displacement to achieved the deformation modes of the adhesively bonded beam. In addition, a finite element model (FEM) is built in the Ls-Dyna software to numerically predict the transverse load displacement of the adhesively bonded beam as well as the delamination between the adhesive layer and metallic adherend (steel U-shape plates). The FEM results agreed well with the experimental results. A parametric study is also carried out to investigate the effects of joint geometrical parameters such as bonded-lap area (or overlap length) and adherend (steel U-shape plates) thickness on the deformation modes and energy absorption performance of the rectangular beam under transverse load.

2. Experimental method

Figure 1 depicts the steel 304L u-shaped plates used to construct the square beam, which were formed using a mechanical press machine and a plastic deformation process. The length, width, height, and thickness of U-shaped sheets are 200, 30, 40, and 1 mm, respectively.
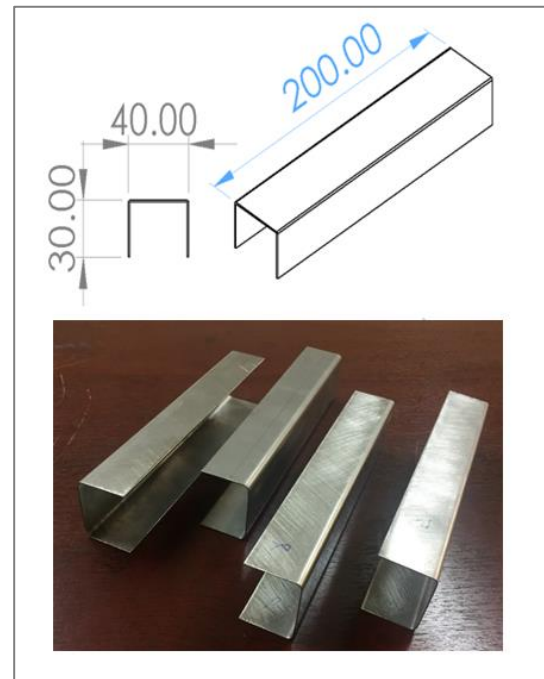

Figure 1: The U-shape steel plates prepared for adhesive bonding

The 3D schematic related to the final assembly of the adhesively bonded thin-walled rectangular beam is shown in Fig. 2. To construct the rectangular beam, two bonding areas, as shown in Fig. 2, should be generated. The surface preparation of adherends is one of the most important factors in the fabrication of adhesive joint structures. The improper surface preparation method results in a weak bond area and, as a result, a lower joint strength. Roughness of the bonded surface can increase bonding area and interfacial forces, resulting in increased mechanical strength for the joint. The metallic adherend's surface was prepared in two steps. The steel adherend was polished in the first step with 400-grit sandpaper at 45 degrees. The bonding surfaces are then washed and cleaned in several steps with 100% industrial acetone and a sterile bandage to remove any fine particles left over from sanding as well as any dust from the experimental setup.
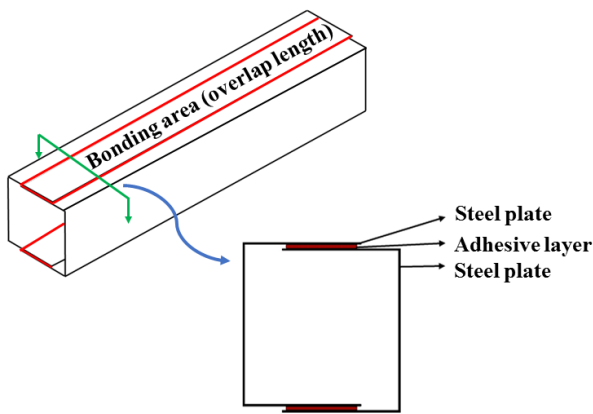
Figure 2: The schematic of the rectangular adhesively-bonded beam in final assembly

Following that, the adhesive should be applied to the bonding surfaces using the manufacturer's recommended 50/50 resin/hardener mixing ratio. In addition, the adhesive layer thickness is controlled by inserting two shims at the fixture's ends.

After one week, all specimens were cured at room temperature. The beam is subjected to 4 mm/min displacement control quasi-static three-point bending load with to scenario. In scenario 1, applied displacement is introduced perpendicular to the overlap length of the beam, whereas in scenario 2, applied displacement is introduced parallel to the overlap length of the beam. These two scenarios are shown schematically in Figure 3.

3. Numerical method

Finite element (FE) analysis was used to numerically investigate the bending behavior of the adhesively bonded steel beam. A quasi-static analysis was performed using commercially available software (LS-DYNA) with explicit temporal integration. Figure 4 depicts the FE model of the steel beam. The steel plates are modeled using shell elements with a reduced element formulation (ELFORM 16), with four integration points considered in the thickness direction. The FE model for steel beams has a total of 17822 elements. For steel beams with geometric dimensions of 200mm*30mm*40mm, a FE mesh with an element size of 1.5 mm was generated.

The effect of mesh density was investigated, and with an element size of 1.5 mm, the FE results for steel beams converge adequately. Interlaminar damage and interface debonding are simulated by an automatic one-way tiebreak contact. These nodes are separable, and the maximum damage is

indicated by the number 1. Section 3.2 describes the delamination failure modeling model in detail. Supporter pins and a moveable punch were created using a rigid material and shell elements. The interaction between the Supporter pins and the moveable punch was assumed to be automatic surface-to-surface contact with a friction coefficient of 0.3. The punch moves quasi-statically downward 0.5 mm per second. The supporter pins were also constrained in all degrees of freedom.
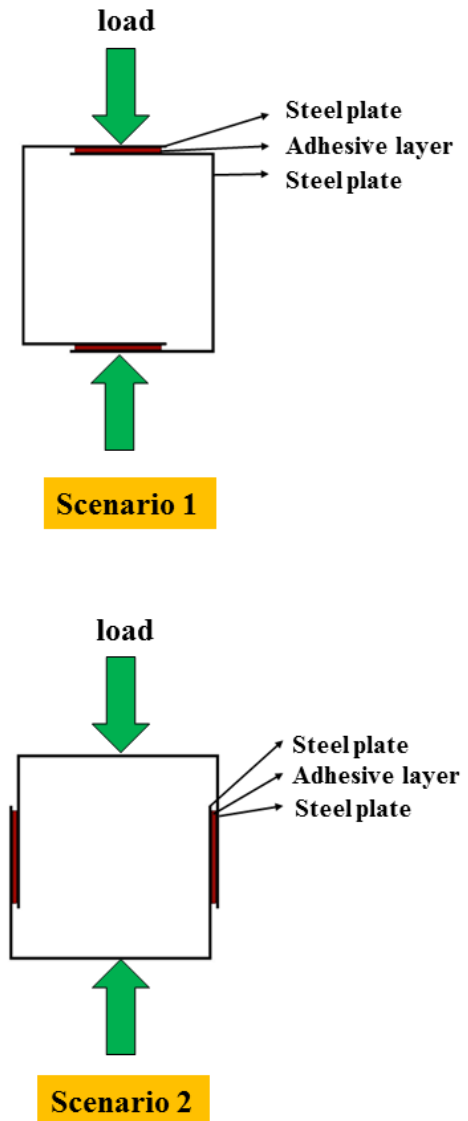

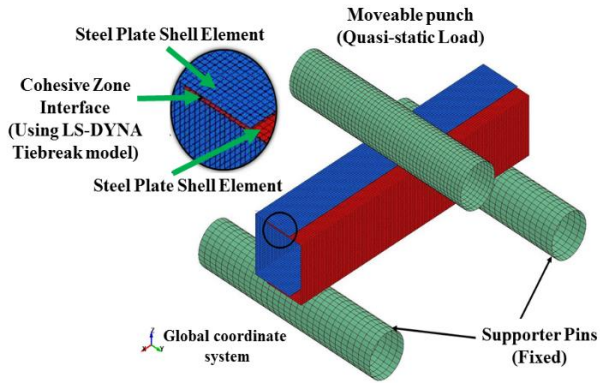**Figure 3:** The schematic of loading scenarios

Figure 4: Description of Finite element model (FEM) of the steel beam

Figure 5: Mixed-mode traction-separation law

Table 1: Delamination damage model input data

Properties	T (MPa)	S (MPa)	G_{IC} (MPa*mm)	G_{IIC} (MPa*mm)
Araldite 2015	15	20	0.359	4.44

3.1. Interface debonding modeling

The interlaminar delamination between the steel layers was modeled using the LS-DYNA cohesive tiebreak algorithms. The shell element layers were tied using a tiebreak contact definition (contact one-way surface to surface tiebreak) with LS-DYNA option 11. This tiebreak model permitted simulation of delamination at the interface of shell element layers. When the stresses at the contact exceed the failure condition, damage occurs:

$$\left(\frac{|\sigma_n|}{NFLS}\right)^2 + \left(\frac{|\sigma_S|}{SFLS}\right)^2 = 1 \tag{1}$$

in which, σ_n and σ_S are the normal and shear stresses acting on the interface, and NFLS and SFLS are the normal and shear strengths of the tie, respectively. After the damage has commenced, the two surfaces begin to separate, and the interfacial stresses decrease as a linear function of the distance between them. According to Figure 5, the Tie brick contact model follows the formulation of the material model MAT COHESIVE MIXED MODE (MAT-138), which follows the traction-separation law of the cohesive zone model. The adhesion properties of the bond between steel layers utilized as input to the tiebreak contact in the simulation are shown in Table 1. G_{IC} is the Mode I energy release; G_{IIC} is the Mode II energy release; T is the peak traction in the normal direction and S is the peak traction in the tangential direction.
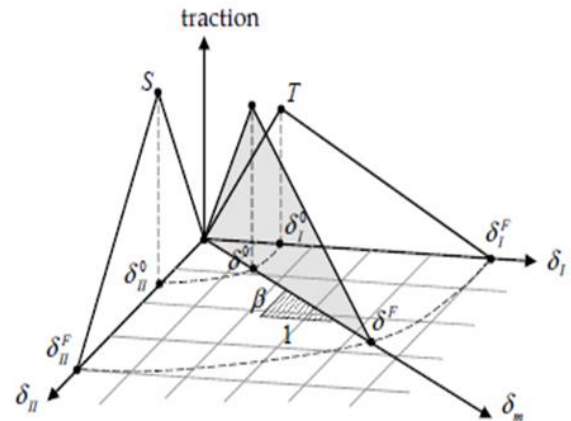
3.2. Steel material model

The Piecewise Linear Plasticity (MAT-24) is an elastoplastic material model with the ability to arbitrarily define the plastic part of the stress-strain plot. n this material model, there is also the ability to define the speed dependence rate. The criterion of failure in this material model is the plastic strain with minimum time step. The plastic areas in this material model are entered according to the actual stress-strain diagram. The strain rate for this material model follows the three theories of Cooper Simonds, Scale yield stress, and viscoelastic formulation, each of these theories can be selected for modeling. In this article, the viscoelastic formulation method is used to predict the behavior of the steel and to activate it, the VP keyword in the (MAT-24) is used, and its value is equal to 1. The mechanical properties of steel extracted from the tensile test [] and entered into the LS-DYNA for simulation according to Table 2.

Table 1: Mechanical properties of Steel 304L

Properties	ρ (kg/m³)	E (GPa)	σ_y (MPa)	σ_u (MPa)	ν
Steel304L	7875	205	310	630	0.3

4. Results

The deformation modes, gradual bending degradation and also the related load-displacement curve of the adhesively bonded rectangular beam is depicted in Figures 4-5 using both experimental and numerical methods. As can be seen, in scenario 2, where the applied load is introduced parallel to the overlap length, a significant delamination has been occurred between the U-shape steel plates and the adhesive layer, however, there is no separation between the adhesive layer and the U-shape steel plates in scenario 1, where the applied load is introduced perpendicular to the overlap length. Furthermore, as shown in Figure 5, the maximum or peak load in scenario 1 is significantly lower than in scenario 2 (25%), which can be considered a key factor in the design of automotive crash box beams that should result in a lower maximum peak load during the collusion process.
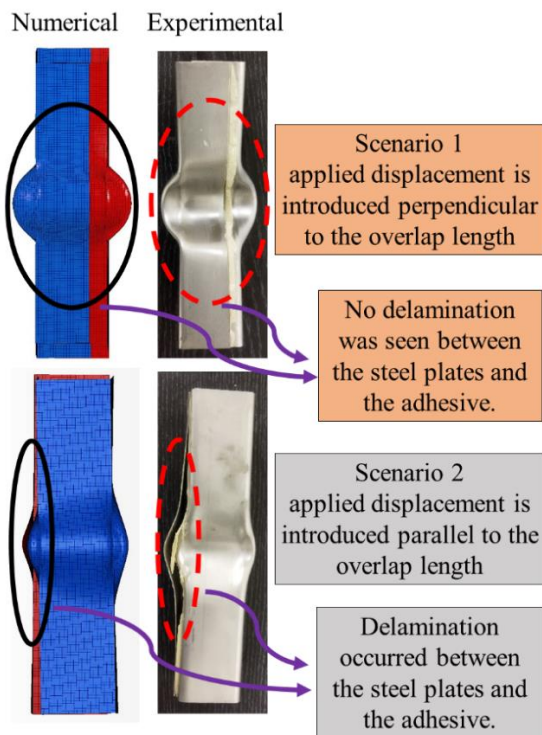

Figure 4: The gradual bending of the adhesively bonded rectangular beam
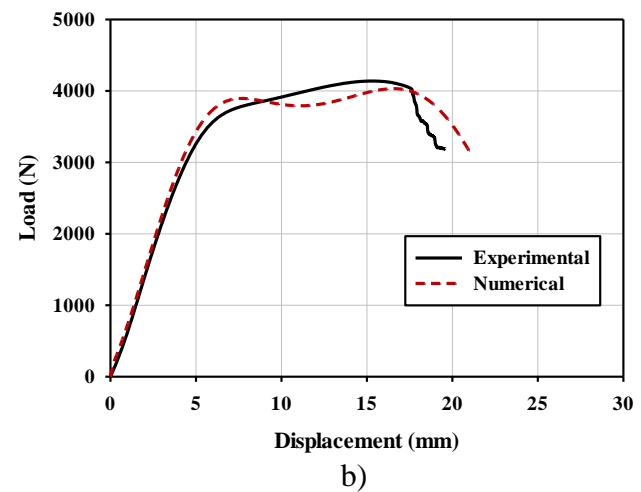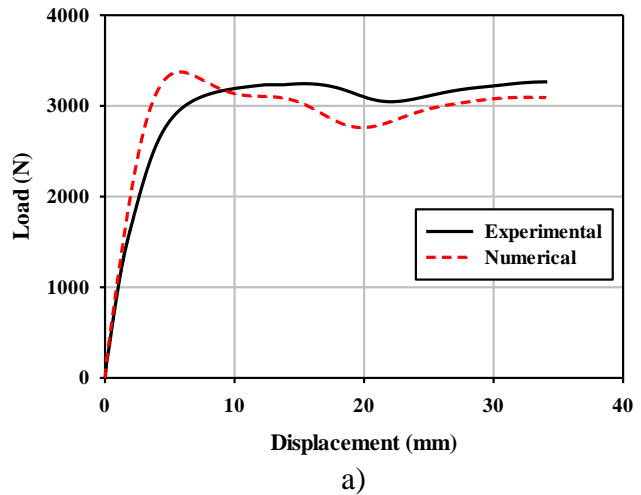

a)

b)

Figure 5: The load vs displacement curves of the rectangular adhesively-bonded beam in a) scenario 1, and b) scenario 2

Moreover, as shown in Figures 4-5, the numerical results have a good accuracy with the experimental results for both deformation modes (Figure 4) and load-displacement curves (Figure 5). As stated in the introduction, the overlap length as well as the thickness of the adherend (U-shape steel plates) have a significant impact on the performance of adhesively bonded structures. In other words, during the loading process, the adhesive layer in the adhesively bonded structures should not fail. In other words, there should be no delamination between the adherend and the adhesive layer. This means that, appropriate thickness for the adherend material as well as the optimal length of bonding area (overlap length) should be determine. Hence, the different values of the U-shape

steel plate thickness and overlap length were investigated in a parametric study using the validated FE model. Figures 6-7 depicts the nodal contact gap contour which represent the occurred damage and subsequently the local and global delamination between the adherend material and adhesive layer. In the FEM prediction of delamination damage, the blue color denotes undamaged areas, the solid red color denotes critical damage, and others represent various damage states. Based on Figure 6, it was found that increasing the thickness of the U-shape steel

plates causes the adhesive layer to delaminate, which led to an incorrect design of the adhesively bonded beam. Figure 7 also illustrates how the length of the overlap affects the probability that the adhesive layer will delaminate. It is obvious that choosing an overlap length that is too small or too large will cause more damage to the adhesive layer and result in an improperly designed adhesively bonded beam.
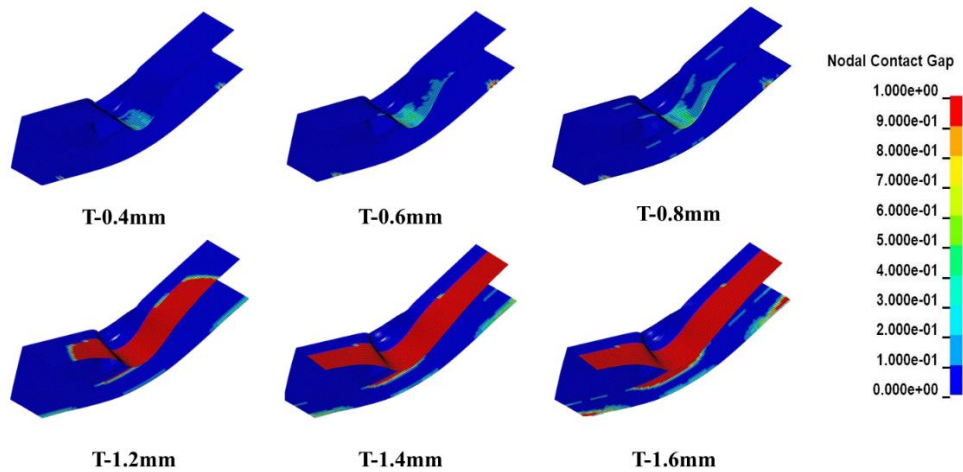

Figure 6: Effect of overlap length on the interfacial delamination between the U-shape steel plates and adhesive layer using the nodal contact gap contour in LS-DYNA
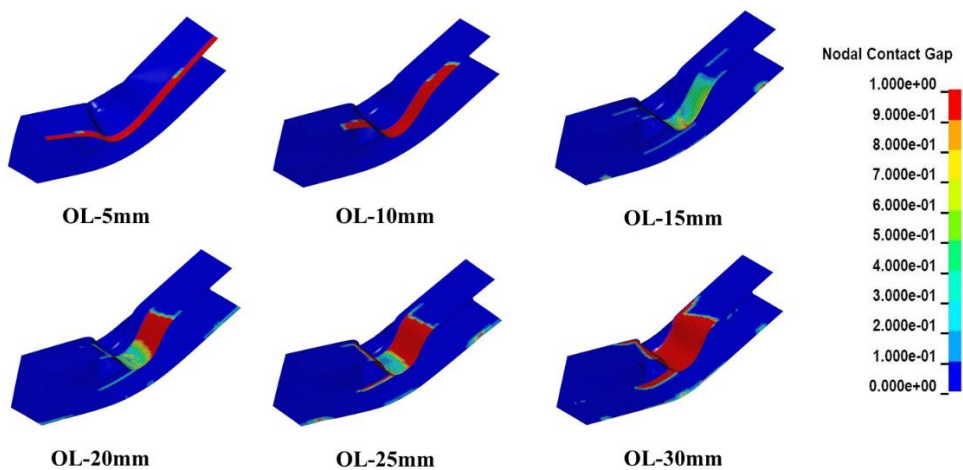

Figure 7: Effect of U-shape steel plate thickness on the interfacial delamination between the U-shape steel plates and adhesive layer using the nodal contact gap contour in LS-DYNA

5. Conclusion

The paper described a gradual degradation process of thin-walled steel adhesively bonded beam with a rectangular cross section subjected to two modes of deformation by three-point bend testing. The study included performing experimental tests and developing a FEA model with damage mechanisms taken into account for the adhesive layer and also plastic collapse for the steel adherend. The three-point bend experimental results were plotted as force-displacement curves and the following structural parameters were assessed: 1) the appropriate loading scenario, 2) the adherend material thickness, and also 3) the overlap length. It was deduced that the adhesively bonded beam exhibits better mechanical performance including greater deformation length when the external load is applied perpendicular to the overlap length. This is in contrast to the case where the external load is applied parallel to the overlap length direction. Also, choosing too small or to big overlap length resulted in damage evolution in the adhesive layer.

List of symbols (Optional)

E	Modulus of elasticity
T	Normal cohesive traction
S	Shear cohesive traction
G_{IC}, G_{IIC}	Mode I, and II fracture energies
ρ	Density of steel material
Greek symbols	
σ_y	Yield stress of steel material
σ_y	Ultimate stress of steel material
ν	Poisson ratio

Reference

[1] P. Reis, F. Antunes, J.J.C.s. Ferreira, Influence of superposition length on mechanical resistance of single-lap adhesive joints, 67 (2005) 125-133.

[2] E.M. Moya-Sanz, I. Ivañez, S.K.J.I.J.o.A. Garcia-Castillo, Adhesives, Effect of the geometry in the strength of single-lap adhesive joints of composite laminates under uniaxial tensile load, 72 (2017) 23-29.

[3] A. Akhavan-Safar, L. Da Silva, M.J.I.J.o.A. Ayatollahi, Adhesives, An investigation on the strength of single lap adhesive joints with a wide range of materials and dimensions using a critical distance approach, 78 (2017) 248-255.

[4] J. Machado, E. Marques, M. Silva, L.F.J.i.J.o.a. da Silva, adhesives, Numerical study of impact behaviour of mixed adhesive single lap joints for the automotive industry, 84 (2018) 92-100.

[5] L.F. Da Silva, R. Carbas, G.W. Critchlow, M. Figueiredo, K.J.I.J.o.A. Brown, Adhesives, Effect of material, geometry, surface treatment and environment on the shear strength of single lap joints, 29 (2009) 621-632.

[6] M. Gheibi, M. Shojaeefard, H.S.J.I.J.o.M.S. Googarchin, Experimental and numerical analysis on the cohesive behavior of an automotive adhesive improved by MWCNT subjected to mode I and II loadings, 153 (2019) 271-286.

[7] M. Gheibi, M. Shojaeefard, H.S.J.E.F.M. Googarchin, A comparative study on the fracture energy determination theories for an automotive structural adhesive: Experimental and numerical investigation, 212 (2019) 13-27.

[8] T. Sadowski, M. Nowicki, D. Pietras, P.J.I.J.o.A. Golewski, Adhesives, Gradual degradation of a thin-walled aluminum adhesive joint with omega cross section under bending, 89 (2019) 72-81.

[9] X. Shang, E. Marques, R. Carbas, A. Barbosa, D. Jiang, L. da Silva, D. Chen, S.J.C.S. Ju, Fracture mechanism of adhesive single-lap joints with composite adherends under quasi-static tension, 251 (2020) 112639.

[10] G. Belingardi, A.J.I.j.o.a. Scattina, adhesives, Experimental investigation on the bending behaviour of hybrid and steel thin walled box beams—The role of adhesive joints, 40 (2013) 31-37.

[11] D.K. Shin, H.C. Kim, J.J.J.C.P.B.E. Lee, Numerical analysis of the damage behavior of an aluminum/CFRP hybrid beam under three point bending, 56 (2014) 397-407.